Proceedings of ASME Turbo Expo 2011
GT2011
June 6-10, 2011, Vancouver, British Columbia, Canada

GT2011-45890

CHARACTERIZATION OF THE AS MANUFACTURED VARIABILITY IN A CVI SIC/SIC WOVEN COMPOSITE

Peter J. Bonacuse
NASA Glenn Research Center
Cleveland, OH, USA

Subodh Mital
University Of Toledo
Cleveland, OH, USA

Robert Goldberg
NASA Glenn Research Center
Cleveland, OH, USA

ABSTRACT

The microstructure of a 2D woven ceramic matrix composite displays significant variability and irregularity. For example, a chemical vapor infiltrated (CVI) SiC/SiC composite exhibits significant amount of porosity arranged in irregular patterns. Furthermore, the fiber tows within a ply frequently have irregular shape and spacing, and the stacked plies are often misaligned and nested within each other. The goal of an ongoing project at NASA Glenn is to investigate the effects of the complex microstructure and its variability on the properties and the durability of the material. One key requirement for this effort is the development of methods to characterize the distribution in as-fabricated ceramic matrix composite (CMC) microstructures with the objective of correlating microstructural distribution parameters with mechanical performance. An initial task in this effort was to perform quantitative image analysis of polished cross sections of CVI SiC/SiC composite specimens. This analysis provided sample distributions of various microstructural composite features, including: inter-tow pore sizes and shapes, transverse sectioned tow sizes and shapes, and within ply tow spacing. This information can then be used to quantify the effect of extreme values of these features on the local stress state with the goal of determining the likelihood of matrix cracking at a given external load.

INTRODUCTION

It has been shown that the local variation in composite microstructure can have a significant effect on some measured bulk properties and the local stress around microstructural features [1,2]. To characterize the microstructural variability the authors have sectioned specimens of ceramic matrix composites composed of eight plies of five harness satin woven SiC fiber tows that was subsequently chemical vapor infiltrated (CVI) with SiC matrix. High resolution images of the microstructure were captured in a sequence of controlled material removal steps. Quantitative image analysis was then used to identify and isolate the fiber tows, pores and matrix. This allowed for the collection of various composite geometric property distributions. The quantitative image analyses performed in this study were accomplished using open-source tools: the Python scripting language [3] and the SciPy and NumPy scientific and numerical libraries [4]. The routines to measure the geometric properties and collect the sample distributions were also written in Python.

SERIAL SECTIONING AND IMAGE ANALYSIS

To capture the variability in the as manufactured microstructure, specimens of an 8 ply, 5 harness satin weave, SiC/SiC CVI composite were serially polished and high resolution images were acquired at each polishing step (Figure 1). The CMC specimens were initially 12.7 mm square with a thickness of approximately 2 mm. The target removal rate was 0.2 mm per polished section. The images were acquired an optical microscope fitted with a two dimensional translating stage and associated control software. 12x3 50x images (each image having 640 by 480 pixel resolution) were acquired for each section and were digitally stitched together. With the high resolution images of the cross section in hand, the task was to develop an automated, objective, and repeatable process to identify the composite constituents. This is a necessary step toward the collection of statistics needed for the generation of analysis models for characterizing the effect of microstructural variability. The process of identifying the portions of an image that have similar characteristics is often referred to as "segmentation". In examining the images it became clear that the image could be 'segmented' into the SiC matrix and fibers, the boron nitride fiber coating, and the epoxy filled porosity. Taking these three image 'segments' as a starting point, algorithms were developed utilizing binary morphological operations (from the SciPy ndimage class) to identify the individual transverse sectioned tows, the longitudinally sectioned tows, the matrix SiC, and the individual inter-tow pores. Figure 1 includes a portion of a polished section and the results of the automated image segmentation and identification process. The software to perform the image segmentation and

quantitative image analysis were written in the Python scripting language [3] using functions from the SciPy library [4]. A full description of the image acquisition and quantitative analysis process is given in [1].

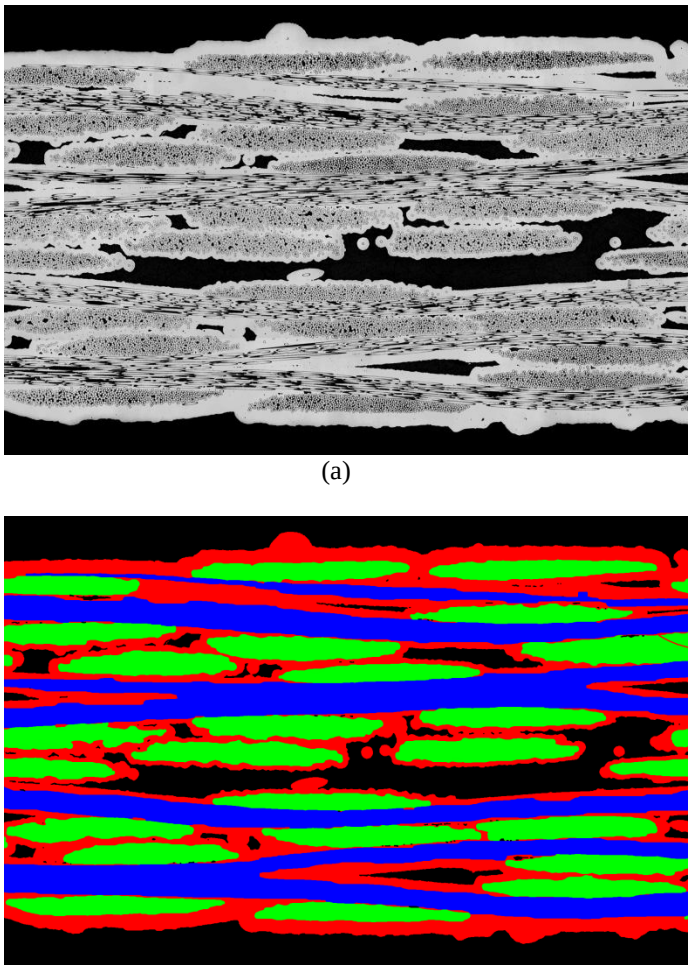

(a)

(b)

Figure 1: A portion of the (a) polished surface of a CVI SiC/SiC composite (50x optical magnification) and (b) the results of automated segmentation and classification (green – transverse sectioned tows; blue – longitudinally sectioned tows; red – SiC matrix; and black – pores)

TRANSVERSE SECTIONED TOWS

After image segmentation and identification of the transverse and longitudinally sectioned tows, the distribution of the size and shape of the transverse sectioned tows was determined. An algorithm was employed that grouped the pixels associated with the transverse sectioned tows by connectivity in order to identify individual tows. Pixels were said to be connected to each other if they shared an edge or a corner. Care was taken to only include complete tows; incomplete tows (tows near the specimen edge that were cut during the fabrication of the specimen) were ignored. Overlapping tows were manually separated by a 1 pixel thin line. Figure 2 shows the distribution of the transverse tow area of the complete tows in a polished section plotted on a normal probability scale. The probability assigned to each data point is derived from the normal order statistic medians of each measured area. The distribution in the area is approximately normal (normally distributed data describe a straight line when plotted on a probability scale) with a coefficient of variation (ratio of the standard deviation to the mean) of about 9%. The distribution in the maximum dimension (width) of the transverse sectioned tows is shown in Figure 3. The distribution of the maximum dimension is approximately normal with a potential outlier at the high end. This long tow was on the specimen surface where the tows tend to be thinner and more elongated due to compression of the ply stack during processing. Figure 4 shows the distribution in the transverse sectioned tow aspect ratio. Note that the range in aspect ratios (from about 6 to greater than 12) indicates a significant variability in the shape of the transverse sectioned tows. The aspect ratio might also be approximated by a normal distribution.

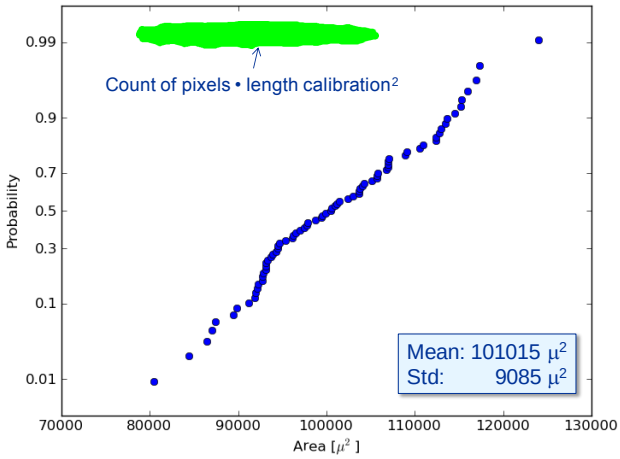

Figure 2: Transverse sectioned tow area sample distribution

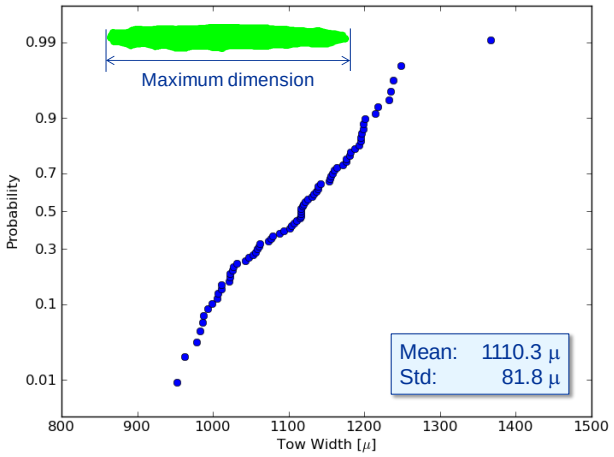

Figure 3: Transverse sectioned tow maximum length sample distribution

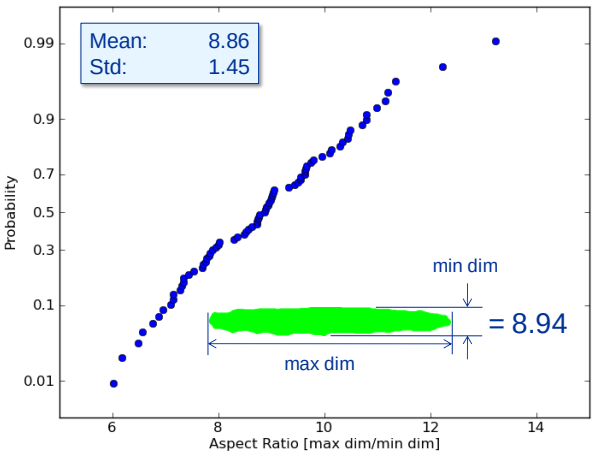

Figure 4: Transverse sectioned tow aspect ratio sample distribution

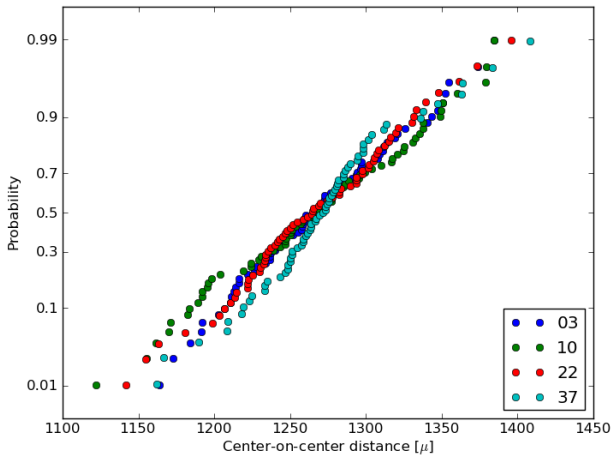

Figure 5: Within ply tow spacing sample distributions for four sections of a CVI SiC/SiC composite specimen

WHITHIN PLY TOW SPACING

To determine the within ply tow spacing distribution, it was first necessary to identify which transverse sectioned tows belonged to each of the eight plies. This would to be a trivial exercise if it were not for the significant intrusion of tows from adjacent plies. An algorithm was devised and tested that can reliably assign the transverse sectioned tows to the appropriate ply. The transverse sectioned tow width is used as an initial estimate of the tow spacing. The algorithm is defined by the following pseudocode:

- Collect statistics on the tow widths
- Find the centroids of all tows (excluding those close to the specimen edge)
- Loop on 8 plies (starting at the bottom of the image)
    - Find the bottom most tow centroid
    - Search left and then right for tows within a range of x-distances (determined by tow width statistics)
        - Find the lowest tow in that range that is not too far removed in the y-direction (as determined by the height of the specimen and number of plies) and add it to the list of tows in the ply
        - Use the tow just found as the next starting point
        - Repeat until there no more full tows that meet the distance criteria (edge of specimen)
    - Once the ply is complete, eliminate tows in the current ply

Probability plots displaying the within ply inter-tow spacing for four sections is displayed in Figure 5. Note that the median tow spacing (intersection of the data with 0.5 probability) for all four sections is close to the expected 1270 micron spacing for the 20 epi woven fabric. Figure 6 is a plot of the data from the four sections as one sample. This plot shows that the within ply tow spacing may be reasonably approximated by a normal distribution.

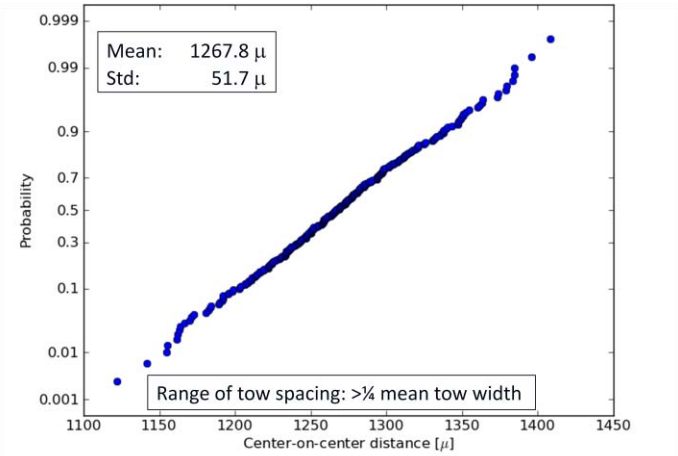

Figure 6: Within ply tow spacing distribution for the combined data set

LONGITUDINAL TOW THICKNESS

The variability of the longitudinal tow thickness observed in the polished sections arises from two sources: the real variation in the tow thickness along its length and the apparent variation due to sectioning of the lenticular cross section tow. Because the tow does not have a uniform cross section, the apparent thickness depends on where, along the width of the tow (the direction perpendicular to the sectioning plane), it is sectioned. If sectioned near the midpoint it will appear to be as thick as the transverse sectioned tows; if sectioned near the edge of the tow it will appear to be significantly thinner. There is also a finite probability that the sectioning plane will fall between two tows in a ply. In addition, due to slight misalignment of the stacked plies relative to the sectioning plane, the apparent thickness of the sectioned longitudinal tow may appear to change as tow transits the image (moving into, or out of, the sectioning plane). In order to measure the apparent average thickness of the longitudinal tows a simple algorithm was devised to sum the height of the longitudinal tows (through the specimen thickness) across the full image and

then divide the mean total height by eight (number of plies in the composite). This average apparent thickness accounts for the variation in the thickness along the length as well as across the tow (lenticular shape).

One can also attempt to collect statistics in the longitudinal tow thickness by sampling the apparent height of the tows in the section images. Note that no attempt was made to separate longitudinally sectioned tows from adjacent plies where they butt up against each other. Figure 7 shows the result of this measurement. As can be seen, there is a wide range in the apparent thickness of the longitudinally sectioned tows. The larger end of the distribution corresponds with twice the thickness of the average transverse tow (mean tow width/mean aspect ratio = 1110.3/8.86 = 125.3 microns) which corresponds to locations where tows from two plies are in direct contact. The thicknesses at lowest end of the distribution (~25 microns and down) corresponds to locations where the sectioning surface barely touches the edge of a tow and is subject to the minimum resolution of the image. This distribution might be approximated by a four parameter truncated normal distribution.

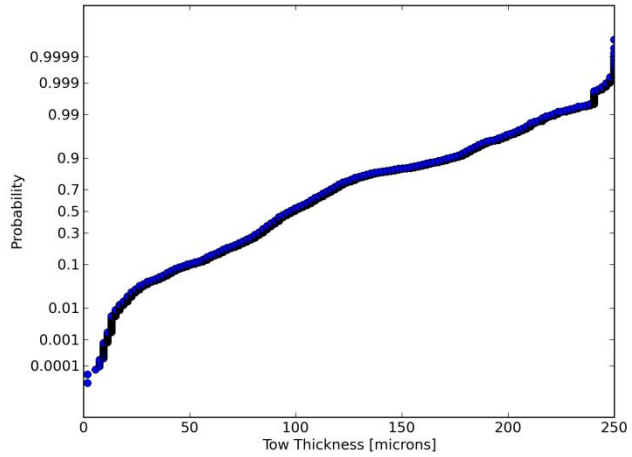

Figure 7: Longitudinal sectioned tow thickness distribution

POROSITY

The inter-tow pores within the CVI composite are highly irregular in shape, size, and location. It has been shown that the shape and size of these pores can have a profound effect on both the across ply stiffness and the local stresses adjacent to the pores. It has also been shown that some extreme values of the pore geometric properties are associated with the highest local stresses in the composite [1]. Higher stresses tend to be located proximate to the larger, higher aspect ratio, pores. Methods were therefore derived to measure and collect several parameters of the pore geometry: area, maximum length, aspect ratio, and a shape factor (compactness) [5]. The area of the pores (Figure 8) can be calculated by simply counting the number of pixels and multiplying by the square of width of the pixel (number of pixels in the pore times the area of a pixel is the area of the pore). The dimensions of the pores can be calculated similarly (distribution of the maximum pore dimension is shown in Figure 9). Aspect ratio and compactness are parameters derived from these calculations (Figures 10 and 11).

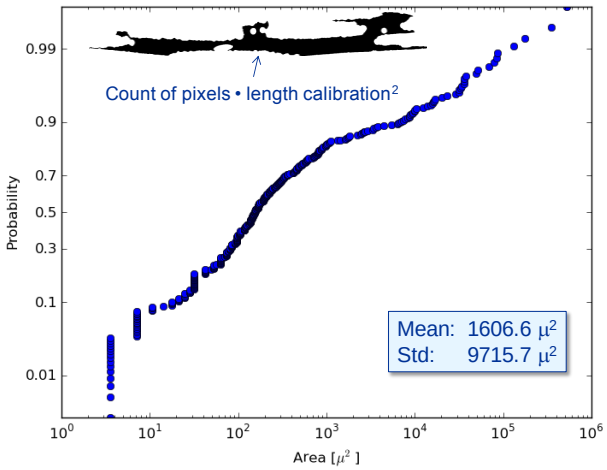

Figure 8: Pore area sample distribution in a CVI CMC section

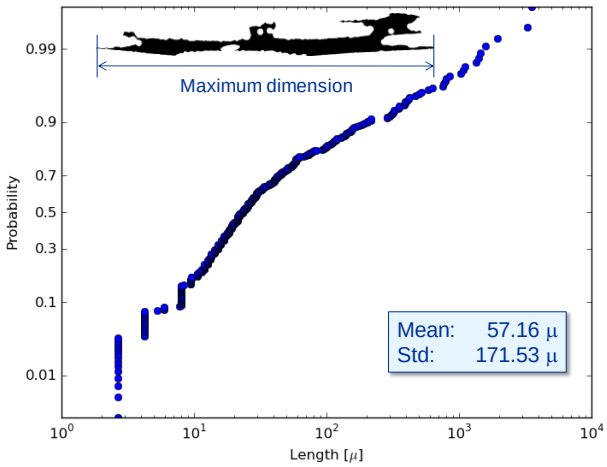

Figure 9: Pore maximum length distribution in a CVI CMC section

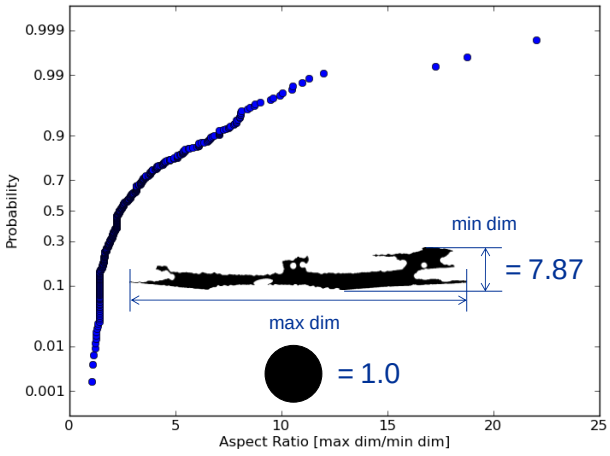

Figure 10: Pore aspect ratio distribution in a CVI CMC

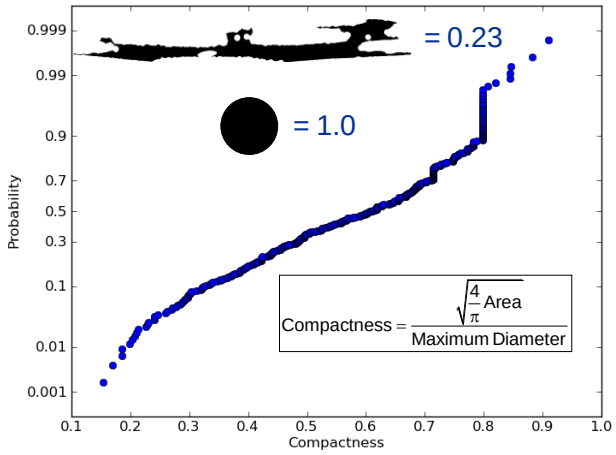

Figure 11: Pore compactness distribution in a CVI CMC

Note that the x-axis scales are logarithmic in Figures 8 and 9 to account for the wide dispersion in the pore areas and lengths. The means and standard deviations in the figures are calculated from the data as collected (no log transformation). The discontinuities in the distributions of the area and length at the low end of the scales is due to the discrete nature of digital imaging (pixel are of finite size). One pixel is 1.88 microns wide and has an area of 3.53 square microns. So the smallest pores in the sample are a single pixel or small clusters of pixels. The distribution in the aspect ratio shows that while many of the pores are not particularly elongated there are a few that are extremely so. The compactness calculation gives an indication of the irregularity of the pore shape with 1.0 corresponding to a circle and smaller values corresponding to increasingly irregular and elongated shapes. It is apparent that the shapes of the pores are varied with some that are highly irregular. The discontinuity in the compactness distribution is again due to the resolution of the digital image. A single pixel (or any square cluster of pixels) will have a compactness of $\sqrt{2/\pi} \approx 0.8$ which corresponds to the large discontinuity in the distribution. The pore area and maximum lengths appear to have bimodal log-normal distributions. Two truncated log-normal distributions might be utilized to approximate the bimodal nature of these sample distributions.

The measured variability in the pore size and shape is a strong indication that treating the porosity as uniformly dispersed in the matrix is an assumption that is unlikely to produce accurate results for some properties, i.e. transverse stiffness, peak local stress, etc..

DISCUSSION

Because there is inherent variability in the composite microstructure the choice of the size of a "representative volume element" or RVE must be larger than the repeating unit cell size in a composite ply (in the case of a five harness satin weave, a 5x5 tow square). The RVE must be large enough to include a statistically significant percentage of the inherent variability. Swaninathan, et al. [6], have introduced the concept of a statistically equivalent representative volume element (SERVE) that sets the RVE size sufficiently large such that some measurement of the microstructural variability does not change significantly from one RVE to the next.

Further study of the relationship between the variability in the local stress and the observed variability in the microstructure is necessary. Ideally, a strong correlation between the observed distribution in the microstructure and the distribution in the local stresses would be found such that inferences about the stress distribution could be made from microstructural observations. The exploration of the local stress in CMC's and its relation to the local geometry is the subject of a paper included in this volume [7].

In addition to the presumed usefulness in determining the size of the SERVE, the distributions of the composite microstructural parameters are to be used to parameterize simulations of composites with realistic variability with the goal of quantifying: the effect of various microstructural features on the local stress state and the probability of extreme values of mechanical properties and local stresses.

While the two dimensional representation of the composite can provide insight into the distribution of local stress in the presence of composite defects, a three dimensional representation must be available to test the utility of the 2D models.

SUMMARY

The variability in CVI SiC/SiC composite microstructure can be characterized from images of polished sections. Automated image processing techniques were employed to segment, identify, and quantify the composite constituents (transverse and longitudinally sectioned fiber tows, SiC matrix, and pores). A number of parameters may be used to quantify the inherent variability in the composite microstructure, a few of which are described and quantified.

ACKNOWLEDGMENTS

The authors wish to acknowledge the hard work of intern Sara Caruso and metallographer Joy Beuhler in polishing the CMC specimens and acquiring the images.

REFERENCES

[1] Goldberg, R. K.; Bonacuse, P. J.; and Mital, S. K.: "Investigation of Effects of Material Architecture on the Elastic Response of a Woven Ceramic Matrix Composite," NASA Technical Memorandum – in preparation.

[2] Morscher, G.N.; DiCarlo, J.A.; Kiser, J.D.; and Yun, H.M.: "Effects of Fiber Architecture on Matrix Cracking for Melt-Infiltrated SiC/SiC Composites", International Journal of Applied Ceramic Technology, Vo. 7, pp. 276-290, 2010.

[3] "Python Programming Language – Official Website", http://www.python.org/

[4] “SciPy.org - Scientific Tools for Python”, http://www.scipy.org/
[5] Russ, John C., “The Image Processing Handbook,” fifth edition, CRC Press, 2007, pp. 581-585
[6] Swaminathan, S.; Ghosh, G.; and Pagano, N. J.: “Statistically Equivalent Representative Volume Elements for Unidirectional Composite Microstructures,” J. of Composite Materials, April 2006, vol. 40, no. 7, pp. 583-604
[7] Subodh K. Mital, Robert K. Goldberg, and Peter J. Bonacuse, “Two-Dimensional Nonlinear Finite Element Analysis of CMC Microstructures,” in Proceedings of ASME Turbo Expo 2011, GT2011, June 6-10, 2011, Vancouver, Canada